Numerical Study of Difference Turbulence Models in a 2D Pipe using and Finite Element Framework

*Naman Agarwal

Abstract

A majority of the processes in nature and industry exhibit turbulence. Hence, understanding turbulence is critical in optimizing different flow behaviour in various petrochemical and bioprocess industries. The present work compares two different turbulence models - LES and RANS - in a 2D pipe with turbulent regime using finite element approach. The results clearly signifies the use of LES turbulence model for better accuracy.

Keywords: Turbulence, Pipe flow, Large eddy simulation, Finite element method

1. Introduction

Turbulence is predominantly observed in many natural and industrial activities. They are defined by high Reynolds number flow which shows chaotic behaviour in the flow resulting in unpredictable pattern of flow fields. Computational fluid dynamics (CFD) is used in the work which is an efficient and economical alternative to experimental investigations for capturing turbulence to its maximum.

The turbulence model widely used in the industry is the Reynolds-averaged Navier-Stokes equation (RANS) model. They are economical by have limited accuracy due to their simplifying assumptions. Large eddy simulation (LES) uses filtered decomposition principle to resolve large scales of motion.

The present work focuses on the CFD modelling of turbulent flow with the use of both LES and RANS model.

The velocity profile in a pipe was initially experimentally studied for a Reynolds number of 4.0×10^5 by Abbott & Kline (1962) and the mean velocity showed an excellent agreement with turbulent at plate profile. A similar study was performed by Barbin & Jones (1963).The previous work on turbulent flow profiles was contradicted by Adrian et al. (1994) for Re = 7000 with a profile different from the logarithmic distribution. The variation was significant at the center of the pipe. Hence, the numerical study was performed for Re =7000 to compare different turbulence models and effect of wall resolution.

2. Methodology

2.1. Flow Equations

The basic mass conservation equation of incompressible flow is:

$$\nabla \cdot \mathbf{u}_i = 0, \qquad (1)$$

The momentum equation describing turbulence is described as:

$$\frac{\partial \mathbf{u}_i}{\partial t} + \mathbf{u}_i \cdot \nabla \mathbf{u}_i + \frac{1}{\rho}\nabla p - \nabla \cdot [\bar{\bar{\tau}}_i] = 0, \qquad (2)$$

where u_i is the phase velocity in spatial direction, ρ is the density, p is the static pressure, $\bar{\bar{T}}_i$ is the shear stress tensor. The filtered and the sub-filtered components using LES model principle are given by (Bull, 2013):

$$\overline{\mathbf{u}} = G \star \mathbf{u}(\mathbf{x}, t) = \int_{-\infty}^{\infty} G(\mathbf{r})\mathbf{u}(\mathbf{x} - \mathbf{r}, t)\mathrm{d}\mathbf{r}, \qquad (3)$$

$$\mathbf{u} = \overline{\mathbf{u}} + \mathbf{u}', \qquad (4)$$

Here, G(r) is the filter kernel and r is the radial distance that is associated with the filter. The sub-filtered interactions results in the sub-filter-scale (SFS) stress whose spherical part is added to the pressure field and the deviatory part, $\bar{\bar{T}}_i{}^{SFS}$

tensor, is modeled using eddy viscosity hypothesis. The resulting filtered momentum equation for phase *i* is given as:

$$\frac{\partial \overline{\mathbf{u}}_i}{\partial t} + \overline{\mathbf{u}}_i \cdot \nabla \overline{\mathbf{u}}_i + \frac{1}{\rho}\nabla \overline{p} - \nabla \cdot [(\bar{\bar{\tau}}_i + \bar{\bar{\tau}}_i^{\mathrm{SFS}})] = 0, \quad (5)$$

SFS stress is modeled using the Boussinesq eddy viscosity hypothesis which is given as:

$$\bar{\bar{\tau}}^{\mathrm{SFS}} = -2\nu_T \bar{\bar{S}}, \qquad (6)$$

where

$$\bar{\bar{S}} = \frac{1}{2}\Big(\nabla \overline{\mathbf{u}} + (\nabla \overline{\mathbf{u}})^T\Big). \qquad (7)$$

Here ν_T is the eddy viscosity is a flow property and is modeled using different LES models.

Second-order Smagorinsky model

The second-order Smagorinsky model is based on Boussinesq hypothesis and assumed between the production and the dissipation rate of SFS kinetic

energy. The eddy viscosity (ν_T) in this model is formulated as:

$$\nu_T = C_s^2 \overline{\Delta}^2 |\overline{S}|, \qquad (8)$$

where C_s is the Smagorinsky constant and [S] is the rate of strain modulus, defined as:

$$|\overline{S}| = \sqrt{2\overline{\overline{S}} : \overline{\overline{S}}}. \qquad (9)$$

The value of C_s varies between 0:1 to 0:17 for shear flows to satisfy the Kolmogorov -5/3 energy law (Pope, 2000).

2.2. Finite element formulation

The SFS stress term is modeled using the Boussinesq eddy viscosity hypothesis leading to the modeled equation as:

$$\frac{\partial \overline{\mathrm{u}}}{\partial t} + \overline{\mathrm{u}} \cdot \nabla \overline{\mathrm{u}} = -\frac{1}{\rho} \nabla \overline{p} + (\nu + \nu_T) \nabla^2 \overline{\mathrm{u}}. \qquad (10)$$

A weak form of the filtered momentum equation is derived by “multiplying" it with a test function $\widetilde{\omega}$ and integrating it over the volume Ω, resulting in:

$$\int_\Omega \widetilde{w} \cdot \left(\frac{\partial \overline{\mathrm{u}}}{\partial t} + \overline{\mathrm{u}} \cdot \nabla \overline{\mathrm{u}} + \frac{1}{\rho} \nabla \overline{p} - (\nu + \nu_T) \nabla^2 \overline{\mathrm{u}} \right) \mathrm{d}\Omega = 0. \qquad (11)$$

In the Galerkin FE method, velocity trial and test functions are approximated using the same bases, ϕl, as:

$$\overline{\mathbf{u}} = \sum_{l=1}^{N_{\mathbf{nodes}}} (\overline{u}_l^1 \phi_l \widehat{\mathbf{i}} + \overline{u}_l^2 \phi_l \widehat{\mathbf{j}}) = \sum_{l=1}^{N_{\mathbf{nodes}}} \phi_l \mathbf{u}_l, \qquad (12)$$

and

$$\widetilde{w} = \sum_{l=1}^{N_{\mathbf{nodes}}} (\widetilde{w}_l^1 \phi_l \widehat{\mathbf{i}} + \widetilde{w}_l^2 \phi_l \widehat{\mathbf{j}}) = \sum_{l=1}^{N_{\mathbf{nodes}}} \phi_l w_l. \qquad (13)$$

The basis functions ϕl take a value one at the node l and zero at all other nodes. In the continuous Galerkin (CG) approach, the chosen basis functions are continuous across elements. For illustration, Figure 1 shows continuous piecewise-linear functions for one dimensional (1-D) and 2-D meshes.

Substituting the approximations for velocity, test function the reduced equation is written in a matrix form as:

$$M\frac{\mathrm{d}\underline{\mathrm{u}}}{\mathrm{d}t} + A(\overline{\mathrm{u}})\underline{\mathrm{u}} + C\underline{\mathrm{p}} + K\underline{\mathrm{u}} = 0, \qquad (14)$$

where the mass matrix M, advection matrix A, pressure gradient matrix C and viscosity matrix Kare given by:

$$M = \int_\Omega \phi_k \phi_l \mathrm{d}\Omega, \qquad (15)$$

$$A(\mathbf{u}) = -\int_\Omega \phi_l \overline{\mathbf{u}} \cdot \nabla \phi_k \mathrm{d}\Omega, \qquad (16)$$

$$C = \int_\Omega \frac{1}{\rho} \phi_k \nabla \varphi_l \mathrm{d}\Omega, \qquad (17)$$

$$K = \int_\Omega (\nu + \nu_T)(\nabla \phi_k \cdot \nabla \phi_l) \mathrm{d}\Omega. \qquad (18)$$

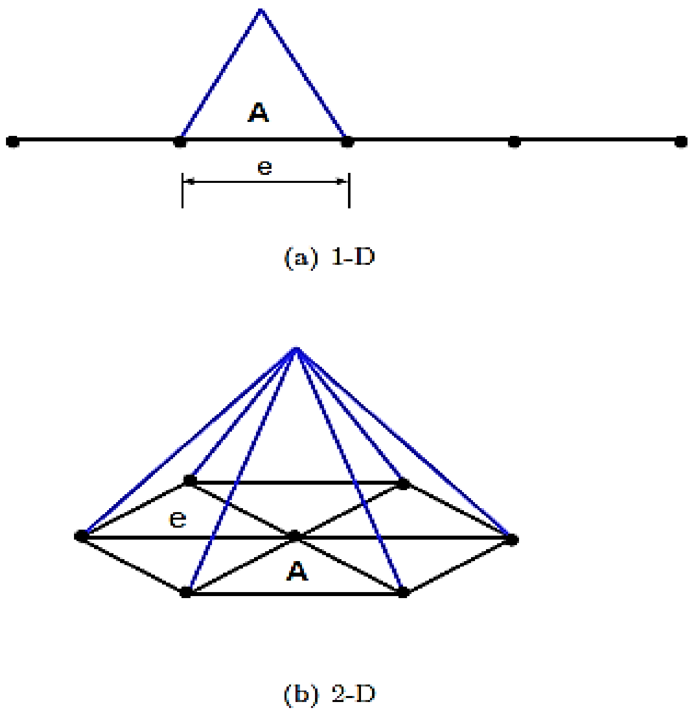

Figure 1: Piecewise-linear continuous finite element basis function with the adjacent nodes is shown for 1-D and 2-D meshes (figure adapted from Wilson (2009).

3. Simulation Setup

The Reynolds number in pipe flow simulations is defined as:

$$Re = \frac{\mathrm{uD}}{\nu}, \qquad (19)$$

where u is the mean velocity in the x-direction developed in the pipe, ν is the kinematic viscosity of the fluid and D is the diameter of the pipe.

The geometry of pipe is schematically represented in Figure 2. The length (L) was sufficiently long for the flow to develop completely.

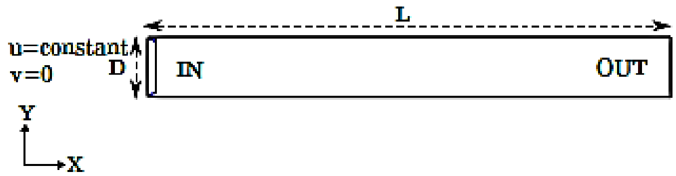

Figure 2: 2D geometry used in pipe flow simulation. L = 200 mm and D = 5:2 mm.

The boundary conditions applied in pipe flow simulations are specified in Table 1.

Table 1: Boundary conditions for 2D pipe flow simulation.

Boundary	Velocity	Pressure
Inlet	u=uniform,v=0	$\frac{\partial p}{\partial n} = 0$
Walls	No slip	$\frac{\partial p}{\partial n} = 0$
Outlet	$\frac{\partial u}{\partial n} = \frac{\partial v}{\partial n} = 0$	p=0

A no-slip boundary condition at the walls and a homogeneous Neumann condition for velocities at the outlet was applied. The flow velocity was initialized to zero for all simulations.

Table 2: Physical parameters for calculating inlet velocity in a 2D pipe flow simulation.

Physical parameter	Value
Reynolds number (Re)	7000
Density ($\mathrm{kg\,m^{-3}}$)	1.225
Diameter (m)	5.2×10^{-3}
Dynamic viscosity ($\mathrm{Pa \cdot s}$)	1.7894×10^{-5}

Table 3: Numerical parameters for 2D pipe flow simulation.

Numerical parameter	Value
Overall simulation time (s)	20
Number of Picard iterations	2
Tolerance for Picard iterations (L^2-norm)	10^{-12}

The physical parameters chosen in the Fluidity framework for current study are stated in Table.

2. The numerical parameters are listed in Table.

3. An implicit scheme was used with a maximum Courant-Friedrichs-Lewy (CFL) number of 0.5 for the simulations. All simulations were executed on a

multicore machine with 20 threads to save on computation time.

4. Results and Discussion

The effect of mesh size on eddy viscosity magnitude and flow dynamics was studied for *Re* = 7000 for three different mesh sizes and was found that velocity

profiles of FM2 mesh with 54475 nodes matched well with the theoretical observations.

4.1. Effect of wall Refinement

Pipe flow simulations were performed with refined mesh at the walls for *Re* = 7000 to study the effect of wall refinement on velocity profile. The mesh was refined to 0.5 mm on both walls of the pipe. Details of the different meshes is stated in Table 4. The meshes are presented in Figure 3.

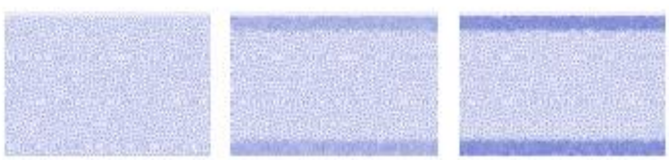

FM2 FM2:WR1 FM2:WR2

Figure 3: Different meshes used in wall resolved 2D pipe flow simulations.

Table 4: Mesh details of different wall resolved cases used in 2D pipe flow simulations.

Table 4: Mesh details of different wall resolved cases used in 2D pipe flow simulations.

Mesh	Mesh size at wall (Δx, mm)	Nodes	Factor ($\frac{\Delta x}{\eta}$)
FM2	0.16	54475	23.6
FM2:WR1	0.08	83525	11.8
FM2:WR2	0.05	133172	7.9

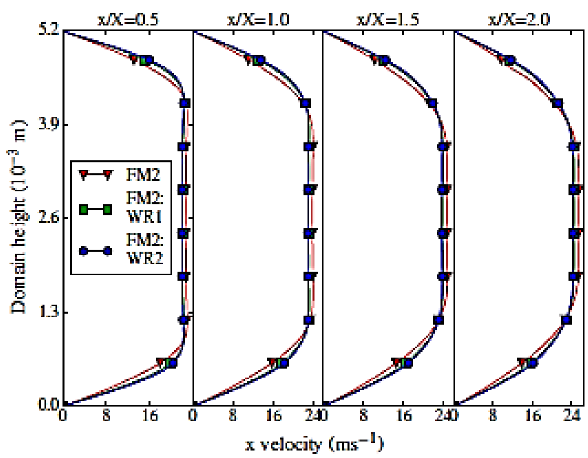

Figure 4: Comparison of velocity profiles for various wall-resolved meshes at different sections in the domain of pipe.

Figure 4 shows a comparison of the velocity profiles at different sections in the domain for different levels of wall refinement. The difference in the velocity between the FM2 and the FM2:WR1 meshes at the center of te pipe was 5%. Hence, wall resolution has a little effect on flow dynamics in the pipe on refining the mesh around the walls. Moreover, the results were similar for FM2:WR1 and FM2:WR2 meshes.

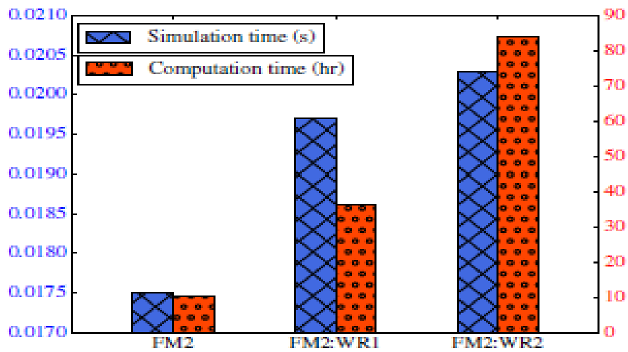

Figure 5: Comparison of computation and simulation time for various wall-resolved meshes after reaching convergence.

The simulation and computation time increased with the increase in number of mesh nodes for the wall refined meshes, as seen in Figure 5. The computation cost of FM2:WR2 mesh was nearly 225% with respect to FM2:WR1 mesh. The FM2:WR1 was chosen along with FM2 mesh to study the effect of using various turbulence models, which is discussed in the next section.

4.2. Effect of different turbulence models

Second-order Smagorinsky LES model and RANS k−ϵ models were compared in this section to study effect of different turbulence models on the flow dynamics in the pipe. RANS model works on the principle of time averaging of velocity and pressure. The mean velocity is calculated as:

$$\mathrm{U}(x,t) = \langle \mathbf{u}(x,t) \rangle = \lim_{T\to\infty} \frac{1}{T} \int_0^T \mathbf{u}(x,t)\mathrm{d}t. \quad (20)$$

The velocity is decomposed into a mean velocity and a fluctuating component, popularly known as the Reynolds decomposition:

$$\mathbf{u}(x,t) = \mathbf{U}(x,t) + \mathbf{u}'(x,t). \qquad (21)$$

The Reynolds Averaged Navier-Stokes equation is the mean momentum equation, expressed as:

$$\frac{\partial \mathbf{U}}{\partial t} + \mathbf{U} \cdot \nabla \mathbf{U} = -\frac{1}{\rho} \nabla \tilde{P} + (\nu + \nu_t) \nabla^2 \mathbf{U}. \quad (22)$$

The eddy viscosity is added to the molecular viscosity to calculate the mean velocity components.

The eddy viscosity is formulated based on Boussinesq eddy viscosity hypothesis and is defined as:

$$\nu_t = C_\mu \frac{k^2}{\epsilon}, \quad (23)$$

where $C\mu$ is a model constant, k represents the turbulent kinetic energy and ϵ is the turbulence dissipation rate. The RANS modeling approach cannot capture the anisotropy of the system and ν_t is a scalar quantity. In the k-ϵ model, separate equations for turbulent kinetic energy and turbulence dissipation rate are solved to obtain the value of eddy viscosity. The turbulent kinetic energy and rate of energy dissipation were initialized to one. The values for k and were set to zero at inlet and walls. A fully-implicit scheme was used to calculate k and ϵ. FM2 and FM2:WR1 meshes were used to run the RANS simulation.

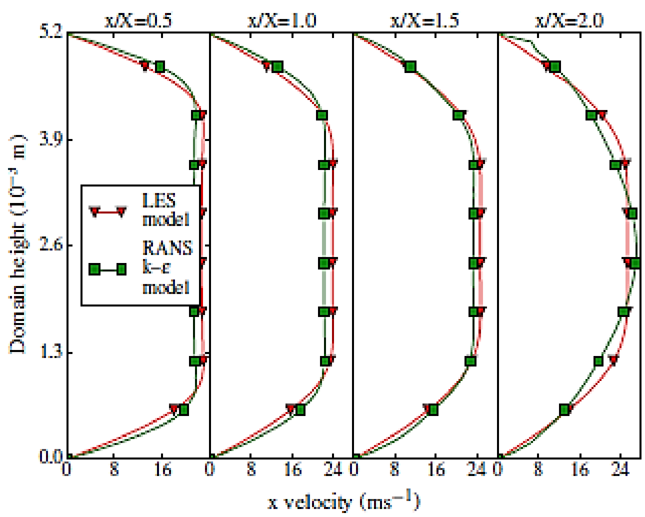

Figure 6: Comparison of velocity profiles for different turbulence models using FM2 mesh in Fluidity.

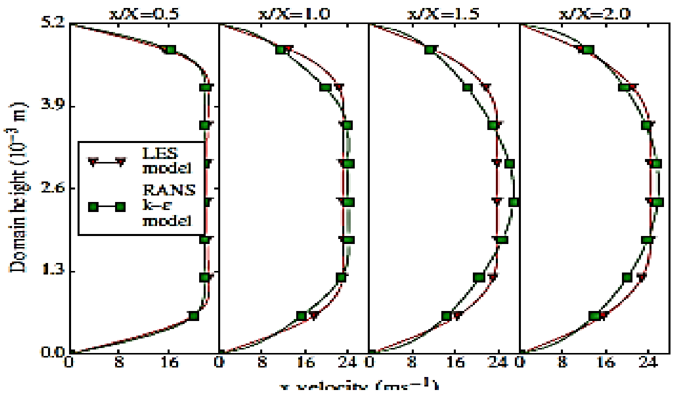

Figure 7: Comparison of velocity profiles for different turbulence models using FM2:WR1 mesh in Fluidity.

Figure 6 shows a comparison of the velocity profiles obtained from different turbulence models at various sections in the pipe for the FM2 mesh. The flow distribution in RANS model did not match well with the LES model. The profile at x/X=2.0 was nearly parabolic for the RANS model. A similar trend was observed for FM2:WR1 mesh, as seen in Figure 7. Hence, LES proved to be better turbulence model to capture flow dynamics in a pipe as it showed flatter profile found in the literature.

5. Conclusion

A comparison of LES and RANS modeling of turbulent flow in a 2D pipe was presented in the work for Reynolds number of 7000. The effect of wall resolution on flow profiles was significant with profile being logarithmic in nature. Further, LES model was tested and compared with RANS model and was proved better in determining the flow behaviour in a pipe with turbulent regime. The present work concludes the effectiveness of LES model for to understand turbulence.

Nomenclature

Abbreviations

2-D	two dimensional
CFD	computational fluid dynamics
CFL	Courant-Friedrichs-Lewy
CG	continuous Galerkin

FE	finite element
HPC	High-performance computing
LES	large eddy simulation
RANS	Reynolds-averaged Navier-Stokes
SFS	sub-filter-scale

Uppercase Roman Symbols

A	advection matrix
C	pressure gradient matrix
$C\mu$	RANS model constant
C_s	Smagorinsky constant
$G_{(r)}$	filter kernel
K	viscosity matrix
L	Length of the domain
M	mass matrix
[S]	rate of strain modulus
$\bar{S}$	filtered rate of strain tensor

Lower Roman Symbols

k	turbulent kinetic energy
p	hydrostatic pressure
$\bar{p}$	modified pressure
r	radial distance associated with the filter
u	velocity
$\bar{u}$	filtered velocity
u'	fluctuating velocity
$\widetilde{w}$	test function

Greek Symbols

ϵ	energy dissipation rate
μ_t	eddy viscosity calculated using RANS model
v_T	eddy viscosity
$\emptyset l$	basis function of velocity
ρ	density
$\bar{\bar{\bar{T}}}$	shear stress tensor
$\bar{\bar{\bar{T}}}^{SFS}$	SFS deviatoric part of SFS tensor
Δx	mesh size
$\bar{\Delta}$	filter width
Ω	computational domain

Mathematical symbols

:	double dot product of two tensors
.	dot product
∇	gradient operator
*	convolution operator

***Research Scholar,**
Multiphase Flow Research Lab,
Indian Institute of Technology Mandi

References

1. Abbott, D. E., & Kline, S. J. (1962). Experimental investigation of subsonic turbulent flow over single and double backward facing steps. Journal of Fluids Engineering, Transactions of the ASME, 84, 317{325.
2. Adrian, R. J., Friedrich, R., & Nieuwstad t, F. T. (1994). Fully developed turbulent pipe flow: A comparison between direct numerical simulation and experiment. Journal of Fluid Mechanics, 268, 175-210.
3. Barbin, A. R., & Jones, J. B. (1963). Turbulent flow in the inlet region of a smooth pipe. Journal of Fluids Engineering, Transactions of the ASME, 85, 29-33. doi:10.1115/1.3656521.

4. Bull, J. (2013). Turbulence Models with Adaptive Meshing for Industrial CFD. Ph.D. thesis Imperial College London.

5. Pope, S. B. (2000). Turbulent flows. Cambridge University Press.

6. Wilson, C. (2009). Modelling multiple-material flows on adaptive unstructured meshes. Ph.D. thesis Imperial College London.